Supplementary material for "Physical and biogeochemical forcing of oxygen and nitrate changes during El Niño/El Viejo and La Niña/La Vieja upper-ocean phases in the tropical eastern South Pacific along 86ºW" by Llanillo et al., 2013.

1) Residuals in mass conservation and robustness of the results.

After running the extended OMP analysis, we only select for our study those points with mass residuals below 4%. It's worthy to remark that the vast majority of the data points present mass residuals considerably below this 4% limit; therefore, the water mass changes described are reliable. In Figure S1 we show the residuals associated to mass conservation in those points selected for our analysis, along both latitude and depth.

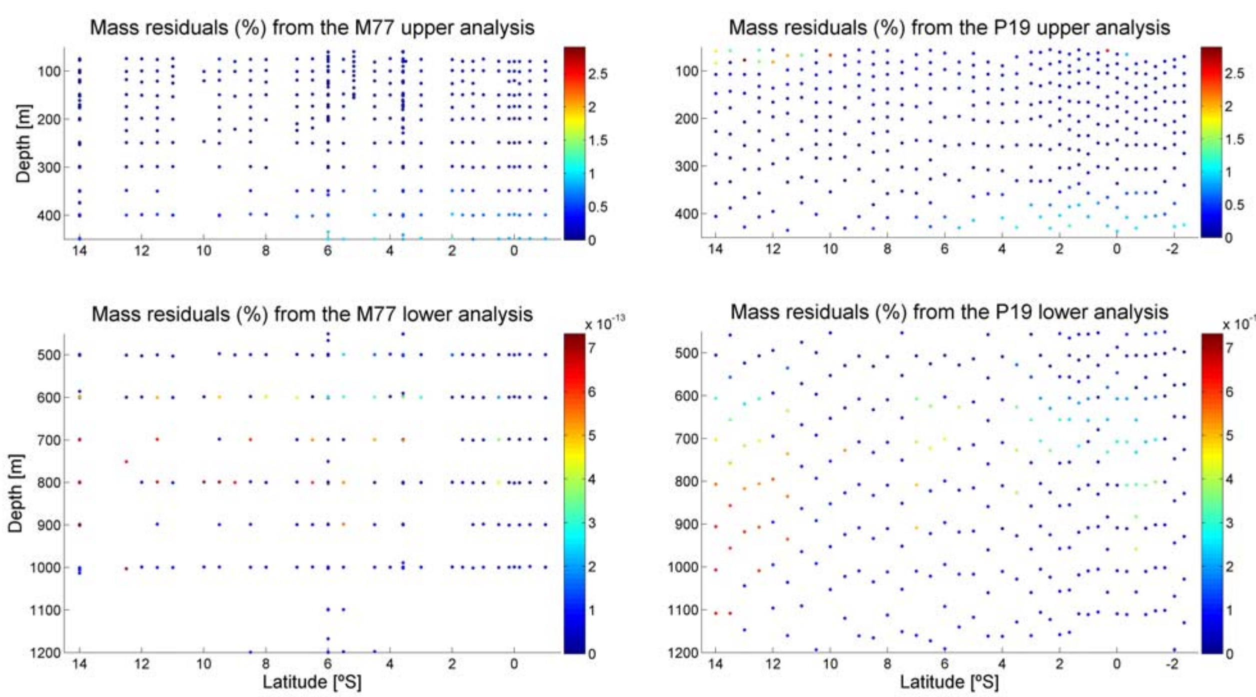

Figure S1. Distribution of the mass conservation residuals (%) for each extended OMP analysis.

2) Assessment of the uncertainty in the water mass mixing fractions as obtained after considering (a) spatial variations in end member properties (natural variability) and (b) temporal variations in end member properties (temporal variability).

We have run a series of sensitivity tests by perturbing simultaneously all water types (end-members) in the source water-mass matrix with a Gaussian noise through a series of Monte Carlo experiments. We have examined what is the influence on the resulting water-mixing fractions.

For the first series of sensitivity tests, we consider the influence of natural variability of each parameter in the source regions where the water types were defined. For this purpose we have calculated the standard error associated to each parameter by averaging the standard errors obtained for such parameter in each source region. These standard errors are then multiplied by the Gaussian noise and the result is added to the corresponding original water type in the source water-mass matrix and then the OMP is solved.

The influence of possible temporal changes of seawater properties in the source regions is considered in a second series of sensitivity tests. We have used the (largest) temporal trends of potential temperature (0.02 ºC/year) and salinity (-0.0005 psu/year) found in the AAIW formation region, in the eastern South Pacific (Schmidtko and Johnson, 2012), to estimate a standard error for the temporal variability of these parameters from 1993 to 2009. We could not find in the literature temporal trends in potential temperature or salinity in the source regions of the remaining water masses so we decided to use the AAIW salinity and potential temperature standard errors for all water masses. We are aware that the AAIW standard errors will probably represent overestimates for the remaining water masses (mainly for ESSW and PDW as they are defined below the sea surface). Therefore, all the results from these sensitivity tests (except for AAIW) must be understood as a 'worst case' scenario, mainly for ESSW and PDW. For all other parameters (nutrients and oxygen) we have used the same standard errors as calculated from the natural variability analysis.

All the above sensitivity tests are run for the upper and lower portions of the P19 and M77 datasets separately. The mixing fractions, obtained for all data points after each perturbed run, are used to obtain average standard errors. Finally, a global-weighted mean standard error is obtained for each water mass mixing fraction (Table S1); the weighting applied takes into consideration the number of data points in each subsection analysed with the OMP method.

Mean standard error (%)	AAIW	ESSW	STW	SAAW	PDW
Natural variability	2.95	9.11	5.32	4.21	7.89
Temporal variability	2.42	7.64	5.08	5.25	4.45

Table S1. Mean standard errors in the water-mass mixing fractions as obtained with the extended OMP analysis after running the sensitivity tests through a series of Monte Carlo simulations.

The global mean standard errors are quite low for AAIW (<3%) under conditions of both natural and temporal variability. This low variability gives us confidence in the results obtained and discussed in this paper. The worst results correspond to ESSW (9%) and PDW (5%). In the case of natural variability this is probably due to the fact that we use the averaged standard error (from all source regions) to characterize the natural variability of each parameter, despite the standard errors in potential temperature and salinity for ESSW and PDW are one or two orders of magnitude smaller than those of the remaining water masses (which were defined at the sea surface). In the case of temporal variability, these relatively large values are related to the fact that we use standard errors that overestimate the temporal change of potential temperature and salinity for these water masses (as explained above).

3) Computation of the best fit between silicate and phosphate (ΔSiO_4: ΔPO_4 ratio).

The ratio ΔSiO_4:ΔPO_4 is affected by the dissolution of opaline silica (Hupe and Karstensen, 2000) and shows regional variations depending on the plankton composition (Poole and Tomczak, 1999). In order to tackle this issue we calculated, for each dataset separately and for both datasets together, the best linear fit (SiO_4 = ratio* PO_4) for the P19 and 774 datasets by means of a linear regression analysis. We then compared the mass residuals produced by the OMP for the different ΔSiO_4:ΔPO_4 ratios.

In Table S2 we compare the goodness of the fit (R^2) and the quality of the OMP solution (mean mass residual in %) for the 40:1 silicate to phosphate ratio (used previously in Llanillo et al., 2012), and for the optimal ΔSiO_4:ΔPO_4 ratios derived from each individual dataset and for both datasets together. We may clearly see that the 40:1 silicate to phosphate ratio produces the worst fit.

Ratio		R^2	Mean mass residual (%)		Std mass residual (%)	
Both	40:1	-	P19	0.4993	P19	0.2977
			M77	0.6273	M77	0.5862
Both	16.61:1	0.4218	P19	0.1397	P19	0.2977
			M77	0.1184	M77	0.1920
M77	14.45:1	0.5741	0.0992		0.1947	
P19	18.37:1	0.5707	0.1233		0.3060	

Table S2. Comparison of the goodness of the fit (R^2) for different linear models between silicate and phosphate, as obtained for different subsets of data points (P19, M77 or both datasets together). The quality of the OMP solution (mean and standard deviation mass residuals in %) is also shown.

According to the info summarized in Table S2, we have selected the ratios (ΔSiO_4:ΔPO_4) obtained for the P19 and M77 datasets (18.37 and 14.45 respectively) because they produce the smallest mean mass conservation residuals while explaining the largest data variability (R^2).

4) Analysis in density space.

We have done an analysis on density space in order to discern the influence of isopycnal heave on the changes described in the paper. Water mass changes in density space are shown in the revised manuscript. Here we show the OMP derived changed in physical transport of oxygen, respired oxygen, physical transport of nitrate, remineralized nitrate and denitrified nitrate (Figure S2).

References:

Hupe, A., and Karstensen, J.: Redfield stoichiometry in Arabian Sea subsurface waters, Global Biogeochem Cy, 14, 357-372, 2000.

Llanillo, P. J., Karstensen, J., Pelegrí, J. L., and Stramma, L.: Physical and biogeochemical forcing of oxygen changes in the tropical eastern South Pacific along 86° W: 1993 versus 2009, Biogeosciences Discuss., 9, 17583-17618, doi:10.5194/bgd-9-17583-2012, 2012.

Poole, R. and Tomczak, M.: Optimum multiparameter analysis of the water mass structure in the Atlantic Ocean thermocline, Deep Sea Res PtI, 46, 1895-1921, 1999.

Schmidtko, S., and Johnson, G. C.: Multidecadal warming and shoaling of Antarctic Intermediate Water, J Climate, 25, 207-221, 2012.

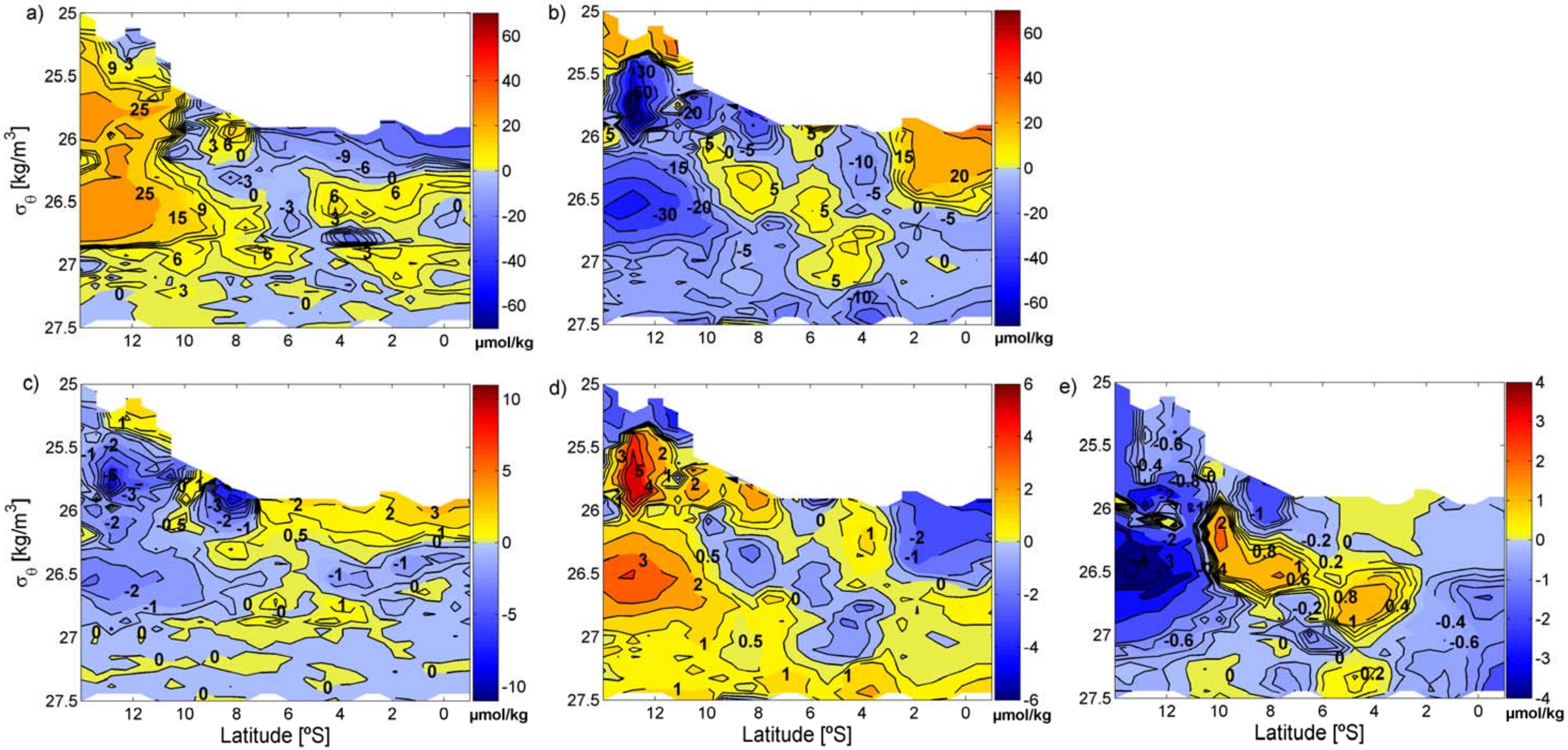

Fig. S2. OMP derived changes in density space between March 1993 and February 2009 (M77-P19): (a) physical transport of oxygen (µmol/kg), (b) respired oxygen (µmol/kg), (c) physical transport of nitrate (µmol/kg), (d) remineralized nitrate (µmol/kg) and (e) denitrified nitrate (µmol/kg).